Am J Cancer Res 2019;9(9):1857-1870
www.ajcr.us /ISSN:2156-6976/ajcr0098920

Review Article

Small molecule TSC01682 inhibits osteosarcoma cell growth by specifically disrupting the CUL4B-DDB1 interaction and decreasing the ubiquitination of CRL4B E3 ligase substrates

Bin Chen[1*], Yu Feng[2*], Meimei Zhang[2], Guangqi Cheng[3], Bin Chen[2], Hantao Wang[2]

Departments of [1]Pharmacy, [2]Orthopaedics, Renji Hospital, School of Medicine, Shanghai Jiao Tong University, Shanghai, China; [3]Department of Orthopaedics, South Campus, Renji Hospital, School of Medicine, Shanghai Jiao Tong University, Shanghai, China. [*]Equal contributors.

Received June 25, 2019; Accepted August 26, 2019; Epub September 1, 2019; Published September 15, 2019

Abstract: The direct interaction between Cullin 4B (CUL4B) and DNA damage-binding protein 1 (DDB1) is required for the assembly of Cullin4B-RING *E3* ligase complex (*CRL4B*), which are involved in the tumorigenesis of osteosarcoma through ubiquitinating and degrading multiple tumor suppressors and cell cycle regulators. Thus, targeting CUL4B-DDB1 interaction to prevent the assembly of CRL4B may be a potent approach to inhibit osteosarcoma cell growth. In the present study, we identified six naturally-sourced small molecules that can specifically disrupt the CUL4B-DDB1 interaction using an *in vitro* high-throughput screening (HTS) system in yeast. We focused our investigation on revealing the molecular effects of TSC01682, the most active compound capable of inhibiting osteosarcoma cell growth. Biochemically, TSC01682 significantly repressed the CUL4B-DDB1 interaction in both yeast cells and osteosarcoma cells. Moreover, TSC01682 treatment in osteosarcoma cells also caused a decrease of other CRL4B components including CUL4-associated factor 11 (DCAF11) and DCAF13, but an increase of two CRL4B substrates including cyclin-dependent kinase inhibitor 1A (CDKN1A, also known as p21) and phosphatase and tensin homolog deleted on chromosome 10 (PTEN) through inhibiting their ubiquitination. Consistent with these molecular changes, TSC01682 treatment significantly inhibited cell proliferation, colony formation, invasion, and *in vivo* tumor growth. Collectively, our results suggest that TSC01682 is a potent compound capable of disrupting the CUL4B-DDB1 interaction, and it may be developed as a chemotherapeutic drug for osteosarcoma treatment.

Keywords: CUL4B, DDB1, small molecule, TSC01628, TSC01131, osteosarcoma

Introduction

Eukaryotic organism genomes encode a class of cullin proteins, which associate with RING proteins to form the largest class of ubiquitin ligases known as the cullin-RING ubiquitin ligases (CRLs) [1, 2]. CRLs are involved in diverse biological processes such as DNA damage and repair, cell cycle progression, apoptosis, and chromatin remodeling through ubiquitinating multiple substrates [2-4]. The human genome encodes eight cullin members, including CUL1, -2, -3, -4A/4B, -5, -7 and -9 [2]. Biochemically, cullin proteins function as scaffolds to recruit RING box proteins (RBX1 and 2), adaptor proteins such as S phase kinase-associated protein 1 (Skp1), elongin B and C, and DNA damage-binding protein 1 (DDB1), and receptor proteins such as F-box proteins and DDB1- and CUL4-associated factors (DCAFs) to assemble different CRLs, which transfer ubiquitin from the RBX1/2-bound E2 to the substrates [2, 5, 6]. It is estimated that the human genome contains more than 600 CRLs [2, 5, 6]. Of these eight cullin genes, the functions of *CUL4A/4B* have been well characterized. Multiple studies have reported that both *CUL4A* and *CUL4B* function as oncogenes in a variety of cancer types including osteosarcoma [7], breast cancer [8], non-small-cell lung cancer (NSCLC) [9], squamous cell carcinoma [10], pleural mesothelioma [11], colorectal cancer

[12], ovarian cancer [13], pancreatic cancer [14], and colitis-associated cancer [15]. Mechanically, CUL4A or CUL4B conservatively associates with DDB1, RBX1 and DCAFs to form multiple CRL4 E3 complexes, which then ubiquitinate numerous substrates, such as the cell cycle regulators CDKN1A (cyclin-dependent kinase inhibitor 1A, also known as p21) and CDKN1B (also known as p27) [16, 17], histone H2A, H3 and H4 [18], and tumor suppressors ST7 (suppression of tumorigenicity 7) and PTEN (phosphatase and tensin homolog deleted on chromosome 10) [15, 19]. Interestingly, the protein sequences of CUL4A and CUL4B share over 80% identity, but they do not show significant functional redundancy. In most cancers, only one of them was observed to be overexpressed, while the other was normal [7-14]. Recently, Liu and colleagues found that both CUL4A and CUL4B were overexpressed in colitis-associated cancer and they could form a heterodimer [15]. Our previous study identified that only CUL4B but not other cullin genes were overexpressed in osteosarcoma [7]. Mechanically, CUL4B acted as a scaffold to directly interact with both DDB1 and RBX1, which associated with two DCAFs including DCAF11 and DCAF13 to assemble two independent E3 ligases known as $CRL4B^{DCAF11}$ and $CRL4B^{DCAF13}$ [7, 19]. Overexpression of CUL4B enhanced the activities of $CRL4B^{DCAF11}$ and $CRL4B^{DCAF13}$ E3 ligases, causing the hyperubiquitination and degradation of their corresponding substrates p21 and PTEN [7, 19]. The downregulation of either p21 and PTEN resulted in the tumorigenesis [7, 19].

Osteosarcoma is a predominantly solid tumor that often occurs in children and young adults [20]. Similar to other cancer types, the current approaches for osteosarcoma treatment include surgery, chemotherapy, and radiation therapy [20]. The chemotherapeutic drugs used often to treat osteosarcoma include doxorubicin, cisplatin, epirubicin, methotrexate, and gemcitabine [21]. Treatments with these spectroscopic medicines often result in chemoresistance after a long period of therapy, which decreases the long-term survival rate of osteosarcoma patients [21]. With the rapid development of personalized medicines in recent years, we also expect to identify small molecules that can specifically target oncogenes involved in the tumorigenesis of osteosarcoma. *In vitro* and *in vivo* experiments in different cancer types have shown that knockdown of CUL4A or CUL4B significantly inhibited tumor cell growth because their knockdown disrupted the stability of CRL4 E3 ligases and caused the accumulation of their substrates [15-19]. These results provide promising evidence that disrupting the assembly of CRL4 E3 ligases may be an effective approach to inhibit tumor cell growth. Given that the assembly of CRL4 E3 ligases is dependent on the direct interactions between DDB1-CUL4 and RBX1-CUL4, we developed an *in vitro* high-throughput screening (HTS) method that utilized the interaction of CUL4B-DDB1 in a yeast system [19]. After screening a small part of compounds in a library containing 40,000 terpenoids sourced from plants and sponges, we obtained one compound TSC01131, which showed a potent cytotoxicity to inhibit the growth of yeast cells and osteosarcoma cells [19]. The promising results encourage us to screen the whole small molecule library to identify more active compounds that specifically prevent CUL4B-DDB1 interaction.

In the present study, we obtained six other compounds showing strong cytotoxicities to inhibit the growth of yeast cells coexpressing CUL4B and DDB1. Of these six compounds, TSC01682 showed the most potent cytotoxicity. We then focused our studies on revealing the molecular effect of TSC01682 on the stability of CRL4B E3 ligases and the ubiquitination of their substrates, as well as evaluating its effect on osteosarcoma cell growth inhibition *in vitro* and *in vivo*. Our results suggest that TSC01682 is a promising candidate for the chemotherapy of osteosarcoma in which CUL4*B* is overexpressed.

Materials and methods

Small molecule screening

Small molecules that disrupted the CUL4B-DDB1 interaction were screened using the same method as described previously [19]. In brief, we primarily constructed two yeast vectors including pGADT7-CUL4B and pGBKT7-DDB1, followed by cotransformed them into AH109 yeast cells and the transformants were selected in the solid synthetic complete (SC) medium without His, Trp and Leu amino acids (SC-HTL). The positive colonies were picked out

after verifying the successful transformation of both DDB1 and CUL4B using western blotting assay. One positive colony was incubated in a 50 mL liquid SC-HTL medium to reach OD_{600} = 1.0. Cells were then diluted 10-fold and equally plated into 96-well plates with a volume of 49 μL, followed by supplementation with 1.0 μL of individual small molecules in each well at a final concentration of 20 μM. The plates were incubated at 30°C for 18 h, and cell density (OD_{600}) was determined using a Synergy HTX Multi-Mode Reader (BioTek, USA). The candidate small molecules that significantly inhibited yeast cell growth were selected based on a standard of OD_{600} < 0.4.

Cell culture and transfection

Two osteosarcoma cell lines, Saos2 (#HTB-85) and MG63 (#CRL-1427), and one osteoblast cell line, hFOB1.19 (#CRL-11372), one colorectal carcinoma cell line HCT-116 (CCL-247), one ovarian cancer cell line SKOV3 (#HTB-77), one gastric cancer cell line MKN45 (#CRL-1739) and one normal colon cell line CCD-18Co (#CRL-1459) were purchased from the American Type Culture Collection (ATCC) (Manassas, VA, USA). Cells were cultured in DMEM (Thermo Fisher Scientific, Waltham, MA, USA, #10569010) supplemented with 10% heat-inactivated fetal bovine serum (FBS) (Thermo Fisher Scientific, #26140079) and 100 U/mL penicillin-streptomycin antibiotics (Thermo Fisher Scientific, #15140148) in a 37°C incubator with 5% CO_2. Plasmid transfection was carried out according to a standard method using Lipofectamine 2000 reagent (Thermo Fisher Scientific, #11668019) [19]. After transfection, cells were incubated at 37°C for 48 h and then used in the required experiments.

Cytotoxicity assay

Yeast cells coexpressing pGADT7-CUL4B and pGBKT7-DDB1 and human cell lines were treated with small molecules including TSC00156, TSC00652, TSC01131, TSC01682, TSC02314, TSC02556, and TSC07432 at different concentrations (0, 1, 2, 4, 8, 16, 32 and 64 μM) for 24 h (yeast cells) and 5 days (human cells), respectively. The density (OD_{600}) of the yeast cells was measured using a Synergy HTX Multi-Mode Reader. The viability of the human cells was determined using an MTT assay kit (Abcam, Cambridge, MA, USA, #ab211091) following the manufacturer's guidelines.

Protein extraction, immunoprecipitation, and western blotting

Yeast protein extracts were prepared by trichloroacetic acid precipitation following a previous protocol [22]. An immunoprecipitation assay in yeast cells was carried out as described previously [19]. Human protein extraction was performed using a standard procedure [19]. In brief, cells were lysed in 1 × radioimmunoprecipitation assay (RIPA) buffer (Cell Signaling Technology, Danvers, MA, USA, #9806S) supplemented with 1 × complete protease cocktail inhibitor (Roche, Basel, Switzerland, #11697498001). Cell lysates were centrifuged at 13000 rpm for 15 min, and the supernatant was denatured at 95°C for 5 min. Equal amounts of proteins from each sample were separated in a 12% SDS-PAGE gel. Immunoprecipitation assay in human cells was carried out as described previously [19]. The primary antibodies were the same as in previous publications [19]. Immunoblot signals were determined using a ChemiDoc MP instrument (Bio-Rad, Hercules, CA, USA).

Flow cytometry assay

Saos2 cells under approximately 70% confluence were treated with 10 μM TSC01131 and TSC01682 at 37°C for 12 h, respectively. Cells were then washed twice with 1 × PBS (phosphate-buffered saline) and then treated with 0.25% trypsin-EDTA (Thermo Fisher Scientific, Cat. #25200056) for 5 min at room temperature. The resulting cells were used for the flow cytometry assay following a previous protocol [7].

Cell proliferation, colony formation, and cell invasion assays

For cell proliferation assay, Saos2 and MG63 cells were treated with 10 μM TSC01131 and TSC01682, respectively. Cell viability was determined at 4 h (0 day), 1, 2, 3, 4 and 5 days using an MTT assay. For colony formation assay, Saos2 and MG63 cells were seeded in 6-well plates with a density of 300 cells per well and then were continuously grown in serum-free DMEM medium supplemented with 10 μM TSC01131 and TSC01682, respectively.

After two weeks, cell colonies were fixed and stained following a previously described method [19]. Cell invasion assay was performed in Boyden chambers. Saos2 and MG63 cells under 80% confluence were suspended in serum-free DMEM medium supplemented with 10 μM TSC01131 or TSC01682 at a density of 5×10^5 cells/mL. The upper chambers were filled with 200 μL cell suspension and the lower chambers were supplemented with 500 μL DMEM containing 10% FBS. The whole sets of chambers were placed in a 37°C incubator for 48 h, and cells on the surface of the lower chambers were fixed with methanol and stained with 0.1% crystal violet.

In vivo tumor formation and growth inhibition assay

Saos2 cells (1×10^6) were suspended in 100 μL of Matrigel Matrix (BD Biosciences, San Jose, CA, USA, #354234) and then diluted with PBS at a 1:1 ratio. Cell suspensions were injected intradermally into the flanks of female athymic *nu/nu* mice (Shanghai SLAC Laboratory Animal Co. Ltd., Shanghai, China). Mice were maintained following the guidelines approved by the Institutional Animal Care and Use Committee (IACUC) of Shanghai Jiao Tong University. At 20 days after the injection, mice with similar tumor volumes (approximately 350 mm^3) were randomly divided into three groups (n = 5 in each group) and then injected with DMSO, 20 μM TSC01131 or 20 μM TSC01682. Tumor volumes were examined with a caliper at 5-day intervals and determined with the formula: Volume = (Length × $Width^2$)/2.

Immunohistochemistry (IHC) assay

IHC staining was performed as described previously [19]. In brief, tumors from mice treated with DMSO, 20 μM TSC01131 and 20 μM TSC01682 were fixed in 10% neutral-buffered formalin (Sigma-Aldrich, St. Louis, MI, USA, #HT501128), and embedded in paraffin. Tissues were sectioned from the midline in five-micrometer-thicknesses. After deparaffinization and antigen retrieval, slides were incubated with anti-CUL4B, anti-DCAF11 and anti-PTEN antibodies, respectively.

Ubiquitination assay

The *in vivo* ubiquitination assay was performed following a previous protocol [19]. Briefly, Saos2 cells were cotransfected with pCDNA3-2 × Flag-PTEN (or pCDNA3-2 × Flag-p21) and pCDNA3-3 × HA-ubiquitin and incubated at 37°C for 48 h. Cells were then resuspended in lysis buffer containing 2% SDS, 150 μM NaCl, 10 mM Tris-HCl (pH 8.0), and 1 × complete protease cocktail inhibitor. After centrifuging at 13000 rpm for 15 min, the supernatant was immunoprecipitated with anti-Flag-agarose resin (Sigma-Aldrich, Cat. #F2426) at 4°C for 2 h. The Flag resin was washed five times with lysis buffer, and equal amounts of protein were loaded in a 12% SDS-PAGE gel for immunoblot analysis using an anti-HA antibody (Abcam, #ab18181).

Statistical analysis

All experiments in this study were repeated three times independently. The statistical analysis of the data was carried out using a two-sided Student's *t* test. Significance was set at $P < 0.05$ (*), $P < 0.01$ (**) and $P < 0.001$ (***).

Results

TSC01628 showed the strongest effect on yeast cell growth inhibition

The promising results of CUL4B and DDB1 knockdown in osteosarcoma cell growth inhibition encouraged us to screen small molecules that specifically targeted the CUL4B-DDB1 interaction [7, 19]. For this purpose, we recently designed and established an HTS method in a yeast system according to the yeast two-hybrid principle in which only cells coexpressing human CUL4B and DDB1 instead of cells harboring CUL4B or DDB1 alone can grow in SC-HTL medium [19]. Using this method, we previously identified a compound TSC01131 in a part of the small molecule library containing 40,000 terpenoids naturally sourced from plants and sponges [19]. TSC01131 showed potent ability to inhibit osteosarcoma cell growth *in vitro* and *in vivo*, and it also could disrupt the CUL4B-DDB1 interaction and decrease the ubiquitination of PTEN [19]. Using the same method, we continued to identify other small molecules in this library. Except for TSC01131, we discovered six other candidate compounds, including TSC00156, TSC00652, TSC01682, TSC02314, TSC02556, and TSC07432 (Supplementary Figure 1). Next, we compared the cytotoxicities of these six compounds in yeast cells coexpressing CUL4B and DDB1

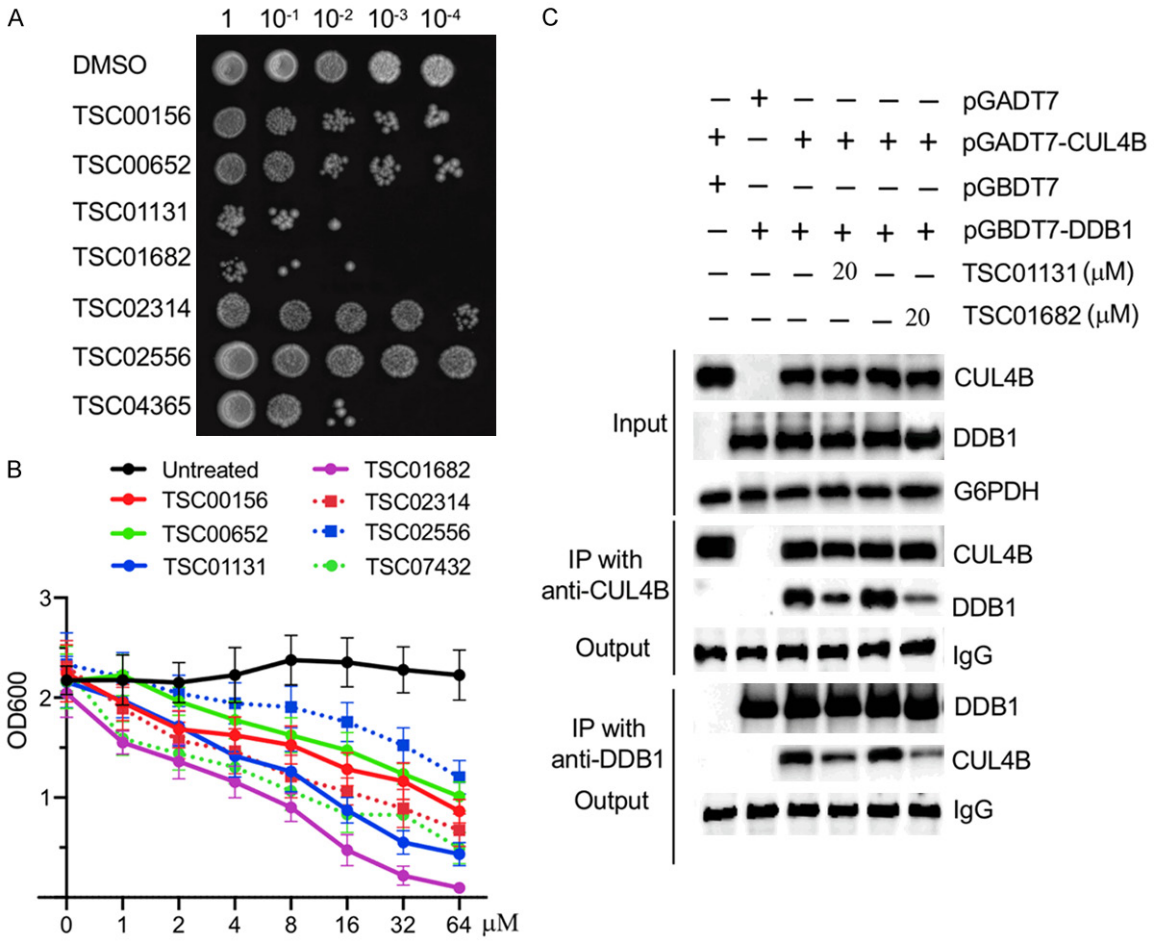

Figure 1. TSC01682 significantly inhibited yeast cell growth through impairing the CUL4B-DDB1 interaction. A. The effects of 20 μM compounds on the growth inhibition of yeast cells. The AH109 yeast cells coexpressing CUL4B and DDB1 were grown to mid-log phase (OD_{600} = 1.0) then mixed with seven compounds (TSC00156, TSC00652, TSC01131, TSC01682, TSC02314, TSC02556, and TSC07432) to a final concentration of 20 μM, respectively. The resulting cells were serially diluted 1-, 10^{-1}-, 10^{-2}-, 10^{-3}- and 10^{-4}-fold, and equal volumes of cells were then dot-plated on a SC-HTL plate. After 72 h of incubation at 30°C, plates were photographed. B. The effects of different concentrations of compounds on the growth inhibition of yeast cells. The AH109 yeast cells coexpressing CUL4B and DDB1 were grown to mid-log phase (OD_{600} = 1.0) and then diluted 10-fold to OD_{600} = 0.1. The resulting cells were grown in SC-HTL liquid medium supplemented with different concentrations (0, 1, 2, 4, 8, 16, 32 and 64 μM) of seven compounds, respectively. After 18 h of incubation at 30°C, the cell density was assessed. *P* values for the comparison of untreated *vs* individual small molecule and TSC01682 *vs* the other individual small molecule were included in Supplementary Table 1. $^{*}P < 0.05$, $^{**}P < 0.01$ and $^{***}P < 0.001$. C. TSC01682 and TSC01131 disrupted the CUL4B-DDB1 interaction. The AH109 cells coexpressing CUL4B and DDB1 were treated with 20 μM TSC01131 or TSC01682 and then subjected to immunoprecipitation assays using anti-CUL4B and anti-DDB1 antibodies, respectively. Cells expressing CUL4B or DDB1 alone were used as controls. After immunoprecipitation, the input and output proteins were detected using anti-CUL4B and anti-DDB1 antibodies, respectively. GAPDH and IgG were used as loading controls.

using TSC01131 as a control. Accordingly, we grew yeast cells *to* mid-log phase (OD_{600} = 1.0) and mixed the cells with different compounds to a final concentration of 20 mM, respectively. After diluting a series of concentrations including 0.1, 0.01, 0.001 and 0.0001 (OD_{600}), cells were dotted on a SC-HTL plate with equal volumes. As shown in **Figure 1A**, these seven compounds exhibited varying cell growth inhibition effects. TSC01682 showed the strongest ability to inhibit cell growth, followed by TSC01131, TSC07432, TSC02314, TSC00156, TSC00652, and TSC02556. We further determined the half-maximal inhibitory concentration (IC50) of these seven compounds. Accordingly, we grew yeast cells in SC-HTL

medium supplemented with a series of chemical concentrations, including 0, 1, 2, 4, 8, 16, 32 and 64 μM. The OD_{600} detection results showed that all of these compounds exhibited a dose-dependent cell growth inhibition effect (**Figure 1B**). The IC50 of these seven compounds were as follows: TSC00156 (57.4 μM), TSC00652 (61.3 μM), TSC01131 (15.6 μM), TSC01682 (7.2 μM), TSC02314 (31.7 μM), TSC02556 (not available due to its range beyond 64 μM), and TSC07432 (30.5 μM). This result further suggested that TSC01682 had the strongest yeast growth inhibition effect among these seven compounds including TSC01131 (**Figure 1B**). Based on these results, our subsequent studies will only focus on TSC01682 and TSC01131, the two most cytotoxic compounds. Because these compounds were obtained based on the principle that they can disrupt the CUL4B-DDB1 interaction, we next aimed to perform an immunoprecipitation assay to determine if TSC01682 and TSC01131 really prevented this interaction. For this purpose, we treated yeast cells coexpressing CUL4B and DDB1 and expressing either CUL4B or DDB1 alone in the conditions with or without small molecules. As shown in **Figure 1C**, we found that neither DDB1 nor CUL4B could effectively pull down each other after small molecule treatments. Moreover, TSC01682 showed a stronger ability to impair the CUL4B-DDB1 interaction (**Figure 1C**). These results suggested that TSC01682 could inhibit yeast cell growth by repressing the CUL4B-DDB1 interaction.

TSC01682 significantly inhibited osteosarcoma cell growth in vitro

Since TSC01682 can significantly prevent the CUL4B-DDB1 association, which may limit the assembly of CRL4B E3 ligases. Thus, we next sought to evaluate whether TSC01682 treatment can inhibit the growth of osteosarcoma cells in which CUL4B was overexpressed. Accordingly, we treated two CUL4B-overexpression osteosarcoma cell lines, Saos2 and MG63, with different concentrations of TSC01682 and TSC01131. Similar to their effects in yeast cells, cell proliferation assay results indicated that both TSC01682 and TSC01131 significantly repressed osteosarcoma cell growth in a dose-dependent manner with an IC50 of 6.2 μM and 15.5 μM, respectively (**Figure 2A** and **2B**). Cell viability was only 6%-10% when cells were treated with 64 μM TSC01682 (**Figure 2A** and **2B**). At the same concentration, cell viability with TSC01131 treatment was 25%-30% (**Figure 2A** and **2B**). Moreover, we also evaluated the molecular changes in the cancer cells treated with different concentrations (0, 2.0, and 20 μM) of TSC01682 or TSC01131. As shown in **Figure 2C** and **2D**, we observed a dramatic decrease of CRL4B components including CUL4B, DDB1, DCAF11, and DCAF13 but a significant increase of their substrates p21 and PTEN in cells treated with TSC01682 or TSC01131. Protein quantification results showed that treatment with 20 μM TSC01131 resulted in a 40%-60% decrease in CRL4B components but a 1.6-2.9-fold increase in p21 and PTEN levels (Supplementary Figure 2). At the same concentration, we observed a 75%-90% reduction in CRL4B components but a 2.5-4.3-fold increase in p21 and PTEN levels in TSC01682-treated cells (Supplementary Figure 2). To evaluate whether the decrease of CRL4B components and the increase of their substrates occurred at the transcriptional level, we also measured mRNA levels of these genes using the same treated cells. Our results indicated that both TSC01682 and TSC01131 treatments did not change mRNA levels of CRL4B components and their substrates (Supplementary Figure 3). These results indicated that TSC01682 was much more active than TSC01131 and these two compounds only affected protein levels of CRL4B components and their substrates but not their mRNA levels.

TSC01682 significantly inhibited the activity of CRL4B E3 ligases

Our pull-down results in yeast cells indicated that TSC01682 treatment caused the impairment of CUL4B-DDB1 interaction (**Figure 1C**). To evaluate whether this was also happened in osteosarcoma cells, we performed an immunoprecipitation assay in Saos2 cells treated with TSC01682 or TSC01131. Interestingly, we observed a significant decrease in CRL4B component protein levels after small molecule treatments (**Figure 3A**, input). Using the same amount of CUL4B or DDB1 as a bait, we can only pull down a small portion of DDB1 or CUL4B in cells treated with small molecules compared to non-treatment (**Figure 3A**, out-

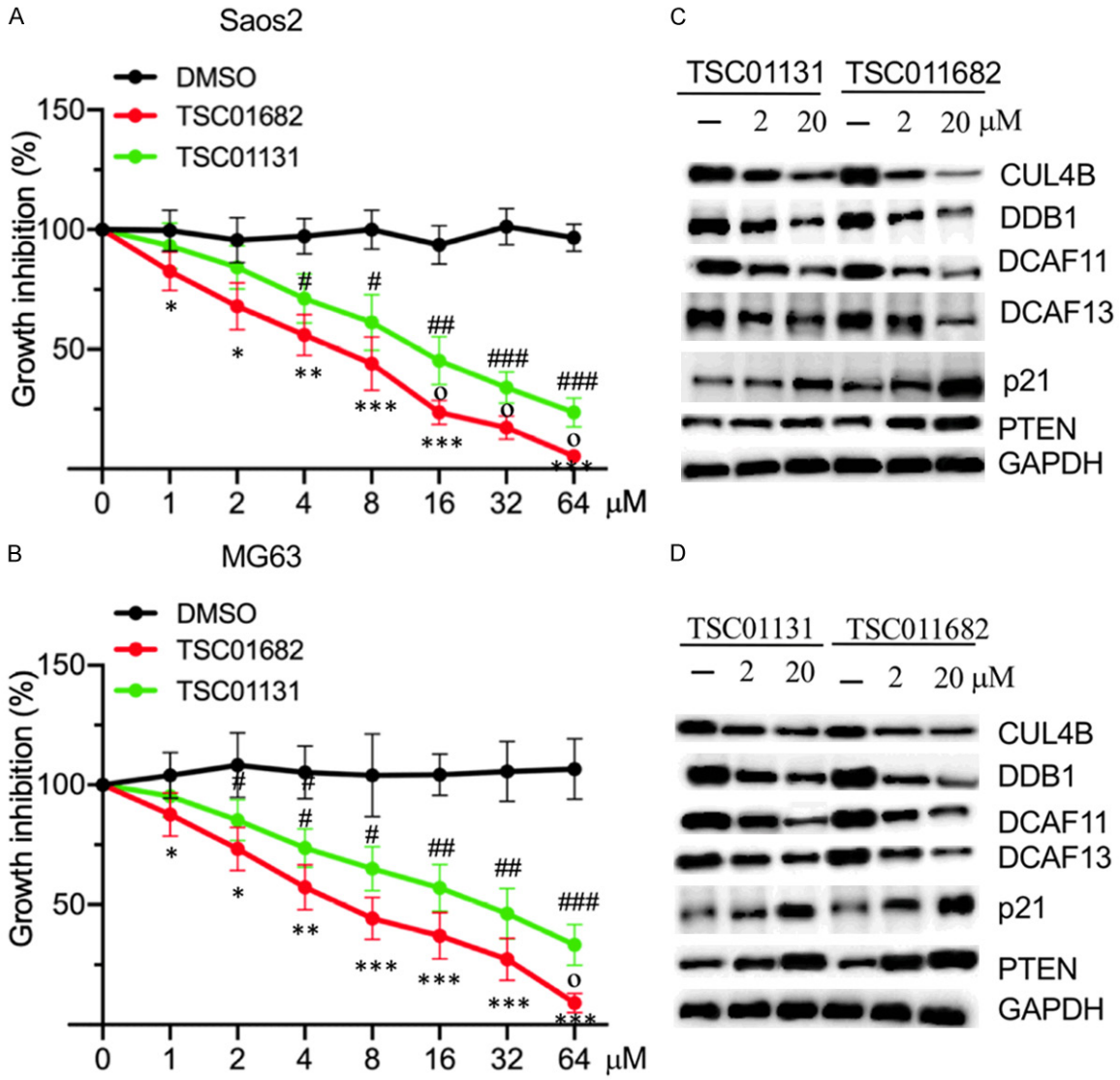

Figure 2. TSC01682 significantly inhibited osteosarcoma cell growth through decreasing protein levels of CRL4B components. (A and B) TSC01682 treatment significantly inhibited osteosarcoma cell growth. Saos2 (A) and MG63 (B) cells were grown in DMEM medium supplemented with different concentrations (0, 1, 2, 4, 8, 16, 32 and 64 μM) of TSC01682 and TSC01131 for 5 days, respectively. Cell viability was determined using an MTT assay. Cell viability without treatment was defined as 100%, and cell viability under other conditions was normalized to that of untreated cells. TSC01131 *vs* DMSO ($^{\#}P < 0.05$, $^{\#\#}P < 0.01$ and $^{\#\#\#}P < 0.001$); TSC01682 *vs* DMSO ($^{*}P < 0.05$, $^{**}P < 0.01$ and $^{***}P < 0.001$); and TSC01131 *vs* TSC01682 ($^{\circ}P < 0.05$). (C and D) The effects of TSC01682 and TSC01131 on protein levels of CRL4B components and their substrates. Saos2 (C) and MG63 cells (D) were treated with 2 μM and 20 μM TSC01682 and TSC01131 for 12 h at 37°C, followed by an examination of the protein levels of CUL4B, DDB1, DCAF11, DCAF13, p21, and PTEN. GAPDH was used as a loading control.

put), which suggested that small molecule treatments significantly disrupted the CUL4B-DDB1 interaction and also caused their degradation in Saos2 cells. Thus, we speculated that the accumulation of p21 and PTEN protein levels after TSC01682 treatment (**Figure 2C** and **2D**) might be resulted from the decrease of their ubiquitination levels. To verify this hypothesis, we expressed different combinations of plasmids including pCDNA3-2 × Flag-PTEN + pCDNA3-3 × HA-Ubiquitin and pCDNA3-2 × Flag-p21 + pCDNA3-3 × HA-Ubiquitin in Saos2 cells. The transfected cells were further treated with or without 20 μM TSC01682 and TSC01131, respectively. The in vivo ubiquitination analysis results showed that both p21 and

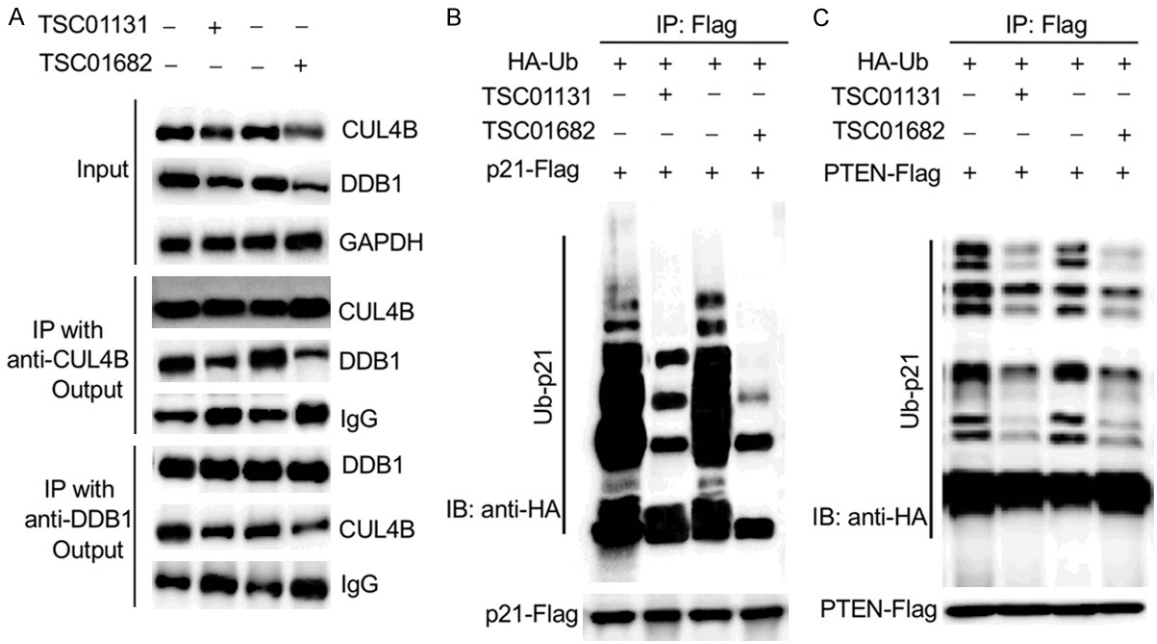

Figure 3. TSC01682 significantly inhibited the ubiquitination of p21 and PTEN. A. TSC01682 treatment significantly decreased the CUL4B-DDB1 interaction in Saos2 cells. Saos2 cells were treated with 20 μM TSC01682 or TSC01131 for 12 h, respectively. The resulting cells were subjected to immunoprecipitation assays using anti-CUL4B and anti-DDB1 antibodies. The input and output proteins were detected using anti-CUL4B and anti-DDB1 antibodies, respectively. GAPDH and IgG were used as loading controls. B and C. TSC01682 significantly inhibited the ubiquitination of p21 and PTEN *in vivo*. Saos2 cells were cotransfected with pCDNA3-2 × Flag-PTEN + pCDNA3-3 × HA-ubiquitin or pCDNA3-2 × Flag-p21 + pCDNA3-3 × HA-ubiquitin and incubated at 37°C for 48 h. Subsequently, cells were treated with 20 μM TSC01682 or TSC01131 for 12 h. The resulting cells were lysed and immunoprecipitated with an anti-Flag antibody to detect loading levels of p21 and PTEN. The blots were also probed with an anti-HA antibody to detect ubiquitinated p21 or PTEN.

PTEN ubiquitination levels were significantly decreased in TSC01682- and TSC01131-treated cells compared to untreated cells (**Figure 3B** and **3C**). In addition, TSC01682 treatment resulted in much lower p21 and PTEN ubiquitination levels than TSC01131 treatment (**Figure 3B** and **3C**). These results demonstrated that two small molecules prevented the CUL4B-DDB1 interaction, resulting in a decrease of CRL4B E3 ligase activities and leading to the accumulation of p21 and PTEN.

TSC01682 treatment impaired cell cycle progression and affected in vitro tumor cell phenotypes

Our previous publications have shown that the downregulation of CRL4B E3 ligase components could decrease the ubiquitination of p21 and PTEN and thus affected cell cycle progression and tumor cell phenotypes [7, 19]. Since small molecule treatments and knockdown of CRL4B components caused similar effects on p21 and PTEN protein levels, we next sought to determine whether TSC01682 treatment also affected cell cycle progression and tumor cell phenotypes such as cell proliferation, cell invasion, and colony formation. Accordingly, we treated Saos2 cells with 20 μM TSC01682 or TSC01131 and analyzed cell cycle distribution by flow cytometry. As expected, our results showed that both TSC01682 and TSC01131 treatments led to a remarkable decrease of the G1 phase but a significant increase of S and G2/M phases (Supplementary Figure 4). Next, we examined the effects of TSC01682 and TSC01131 on the phenotypes of Saos2 and MG63 cells. Accordingly, we treated cells with 10 mM TSC01682 or TSC01131 and then measured cell proliferation at different time points. The MTT assay results indicated that treatment with both TSC01682 or TSC01131 significantly inhibited cell proliferation in comparison to no treatment (**Figure 4A** and **4B**). Using the same concentration, we also evaluated the effects of TSC01682 and TSC01131 on colony formation

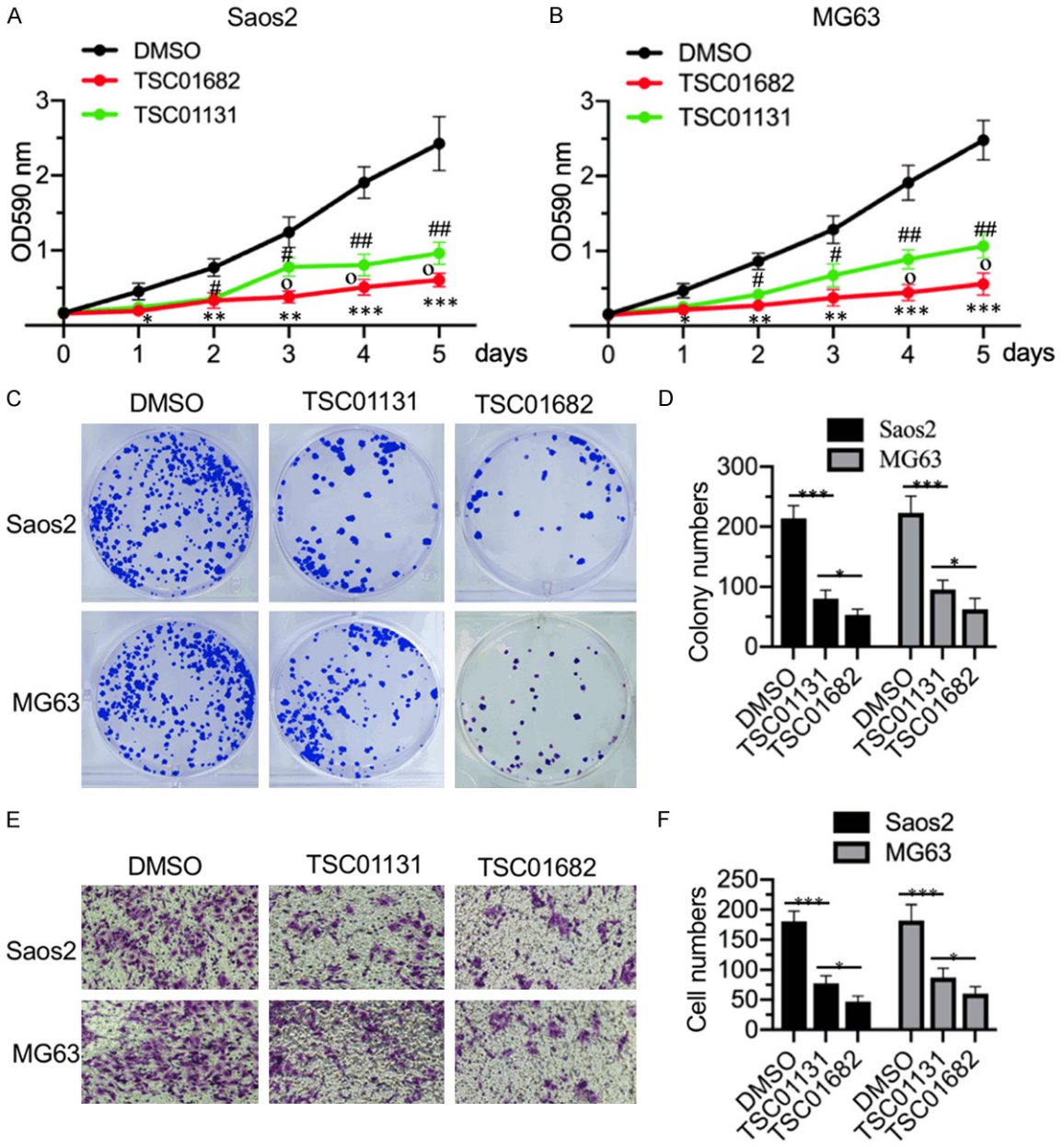

Figure 4. TSC01682 treatment decreased cell proliferation, colony formation, and cell invasion. (A and B) TSC01682 treatment inhibited osteosarcoma cell proliferation. Saos2 (A) and MG63 (B) cells were grown in DMEM medium supplemented with 20 μM TSC01682 and TSC01131 for 5 days. Cells were collected each day and cell viability was assessed using an MTT assay. TSC01131 *vs* DMSO ($^{\#}P < 0.05$ and $^{\#\#}P < 0.01$); TSC01682 *vs* DMSO ($^{*}P < 0.05$, $^{**}P < 0.01$ and $^{***}P < 0.001$); and TSC01131 *vs* TSC01682 ($^{\circ}P < 0.05$). (C and D) TSC01682 treatment inhibited colony formation of osteosarcoma cells. Saos2 and MG63 cells were seeded on six-well plates at a density of 300 cells per well. Cells were grown in serum-free DMEM medium supplemented with 10 μM TSC01131 or TSC01682 and then continuously cultured for two weeks. Colonies were stained with 0.5% crystal violet and photographed (C), and colony numbers were quantified (D). $^{*}P < 0.05$ and $^{***}P < 0.001$. (E and F) TSC01682 inhibited osteosarcoma cell invasion. A total of 1×10^5 cells in each treatment were applied to examine their invasion ability using a Boyden chamber assay. The invading cells were stained with 0.1% crystal violet and photographed (E), and cell numbers were quantified (F). $^{*}P < 0.05$ and $^{***}P < 0.001$.

and cell invasion. Our results showed that treatments with these two compounds significantly decreased colony and invading cell numbers compared to non-treatment (**Figure 4C-F**). By

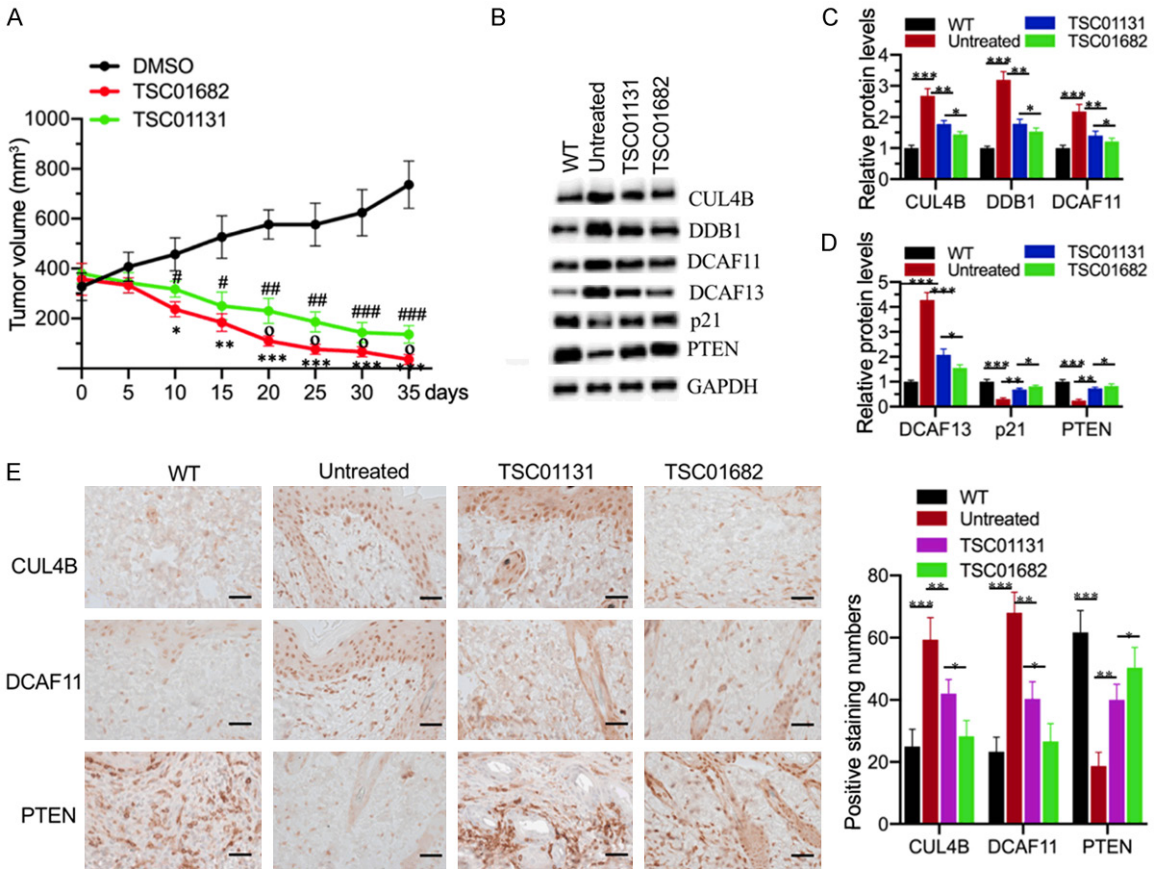

Figure 5. TSC01682 inhibited osteosarcoma tumor growth *in vivo*. (A) TSC01682 treatment eliminated tumors *in vivo*. Saos2 cells were injected intradermally into the flanks of nude mice. On day 20 after injection, mice with similar tumor volumes (approximately 350 mm^3) were randomly divided into three groups (n = 5 in each group) and then injected with DMSO, 20 μM TSC01131 and 20 μM TSC01682, respectively. Tumor volumes were measured with calipers at 5-day intervals. TSC01131 *vs* DMSO ($^{\#}P < 0.0$, $^{\#\#}P < 0.01$ and $^{\#\#\#}P < 0.001$); TSC01682 *vs* DMSO ($^{*}P < 0.05$, $^{**}P < 0.01$ and $^{***}P < 0.001$); and TSC01131 *vs* TSC01682 ($^{\circ}P < 0.05$). (B-D) TSC01682 treatment affected the protein levels of CRL4B components *in vivo*. The nude mice (WT), untreated tumors (untreated), tumors treated with TSC01682 and tumors treated with TSC01131 were lysed and subjected to western blotting to examine the protein levels of CUL4B, DDB1, DCAF11, DCAF13, p21, and PTEN. GAPDH was used as a loading control (B). The relative protein signals were quantified and shown in (C) and (D). $^{*}P < 0.05$, $^{**}P < 0.01$ and $^{***}P < 0.001$. (E) IHC staining. The bone-adjacent tissues from nude mice (WT), untreated tumors (untreated), tumors treated with TSC01682 and tumors treated with TSC01131 were subjected to IHC staining with anti-CUL4B, anti-DCAF11, and anti-PTEN antibodies, respectively. Scale bars = 100 μm. The positive signaling numbers were counted. $^{*}P < 0.05$, $^{**}P < 0.01$ and $^{***}P < 0.001$.

comparing the effects of the two compounds, TSC01682 treatment resulted in a 75% reduction in the colony and invading cell numbers, while TSC01131 treatment caused only a 60% reduction (**Figure 4D** and **4F**). These results consistently supported the conclusion that TSC01682 was much more effective than TSC01131.

TSC01682 treatment significantly inhibited in vivo tumor growth

Our above *in vitro* results consistently indicated that both TSC01682 and TSC01131 significantly inhibited CRL4B E3 ligase activity and tumor cell growth. We next sought to evaluate whether these two compounds had the same suppressive effects *in vivo*. Thus, we primarily injected nude mice with Saos2 cells to generate tumors. After 20 days of injection, mice with similar tumor volumes were grouped and injected with DMSO (control), 20 μM TSC01682 and TSC01131 compounds, respectively. After monitoring for 30 days, we found that mice injected with either TSC01682 or TSC01131 showed a significant decrease in tumor volume compared to mice injected with DMSO (**Figure 5A**). Interestingly, TSC01682 could eliminate

more than 90% of tumors while TSC01131 only eliminated ~75% tumors by the 30th day (**Figure 5A**). Next, we measured the protein levels of CRL4B E3 ligase components and their substrates in the tumor tissues from TSC01682- or TSC01131-treated mice. Consistent with the in vitro results, the protein levels of CUL4B, DDB1, DACF11, and DCAF13 were all significantly decreased, while p21 and PTEN protein levels were remarkably increased after TSC01682 or TSC01131 treatment (**Figure 5B**). Protein quantification results showed that TSC01682 treatment caused a 50%-60% reduction in CRL4B component levels, while TSC01131 treatment resulted in only a 40%-50% reduction in the level of these proteins (**Figure 5C** and **5D**). Moreover, TSC01682 and TSC01131 treatments caused a 75%-85% and a 70%-80% increase in p21 and PTEN levels, respectively (**Figure 5C** and **5D**). Furthermore, we used wild-type (WT) nude mice as a control and found that neither TSC01682 nor TSC01131 treatment could not change the protein levels of CRL4B components and their substrates to a comparable level in WT mice (**Figure 5B-D**). In addition, we analyzed the histological changes in CUL4B, DCAF11 and PTEN after small molecule treatments. Consistent with the immunoblot results, we found that the levels of CUL4B and DCAF11 were significantly decreased, while the PTEN level was remarkably increased after TSC01682 and TSC01131 treatments (**Figure 5E**). These results suggested that TSC01682 had promising *in vivo* effect on eliminating tumors through affecting the assembly of CRL4B E3 ligases.

Discussion

Emerging evidence reveals that CRL4 E3 ligases can ubiquitinate multiple tumor suppressors and cell cycle regulators [7-19]. Increased activities of these E3 ligases driven by CUL4 overexpression cause the degradation of their substrates, leading to tumorigenesis [7-19]. The DDB1-CUL4 interaction is critical for the assembly of CRL4 E3 ligases [7-19]. Thus, targeting CUL4-DDB1 interaction may be an effective strategy to inhibit tumor growth in cancers with CUL4 overexpression. In this study, we compared the cytotoxicity of seven small molecules identified by an *in vitro* HTS method. We focused our experiments on evaluating the molecular effects of TSC01682, the most active compound disrupting the CUL4B-DDB1 interaction. Collectively, our *in vitro* and *in vivo* data support a model in which TSC01682 and TSC01131 treatments markedly reduce the growth of osteosarcoma cells through decreasing CRL4B E3 ligase components and increasing their substrates p21 and PTEN (**Figure 6**). The accumulation of p21 and PTEN can effectively affect cell cycle progression and inhibit tumor cell growth.

CUL4A and CUL4B are two paralogous proteins that share more than 80% amino acid sequence identity [2]. In this study, we only investigated the effects of TSC01682 on osteosarcoma cell growth inhibition and the molecular changes of CRL4B components and their substrates. Since CUL4A and CUL4B are highly conserved, we speculate that TSC01682 should also block the DDB1-CUL4A interaction, which means that TSC01682 should also inhibit the growth of other cancer cells that overexpress CUL4A or CUL4B, not only osteosarcoma cells. To verify this hypothesis, we examined the growth inhibition effect of TSC01682 on three other cancer cell lines overexpressing CUL4A and CUL4B, including a colorectal cancer cell line HCT-116 with CUL4A overexpression [23], an ovarian cancer cell line SKOV3 with CUL4A overexpression [24], and a gastric cancer cell line MKN45 with CUL4B overexpression [25]. As expected, our results showed that the growth of these cells was significantly inhibited by TSC01682 treatment in comparison to non-treatment (Supplementary Figure 5). These results, together with our above results in osteosarcoma cells, clearly suggested that TSC01682 effectively inhibited the growth of cancer cells overexpressing either CUL4A or CUL4B. Given that our screening strategy was based on disrupting the CUL4B-DDB1 interaction, we assumed that all of the other six compounds had similar effects, although their cytotoxicities might vary. Comparing the chemical structures of these seven compounds, it appeared that there was no significant similarity except for their sesterterpenoid structures. Because these compounds are naturally sourced, it is difficult to obtain a large number of small molecules in our materials. We are currently seeking to synthesize these chemicals in our laboratory. Moreover, we are also trying to modify these small molecules and synthesize their derivatives in order to obtain compounds

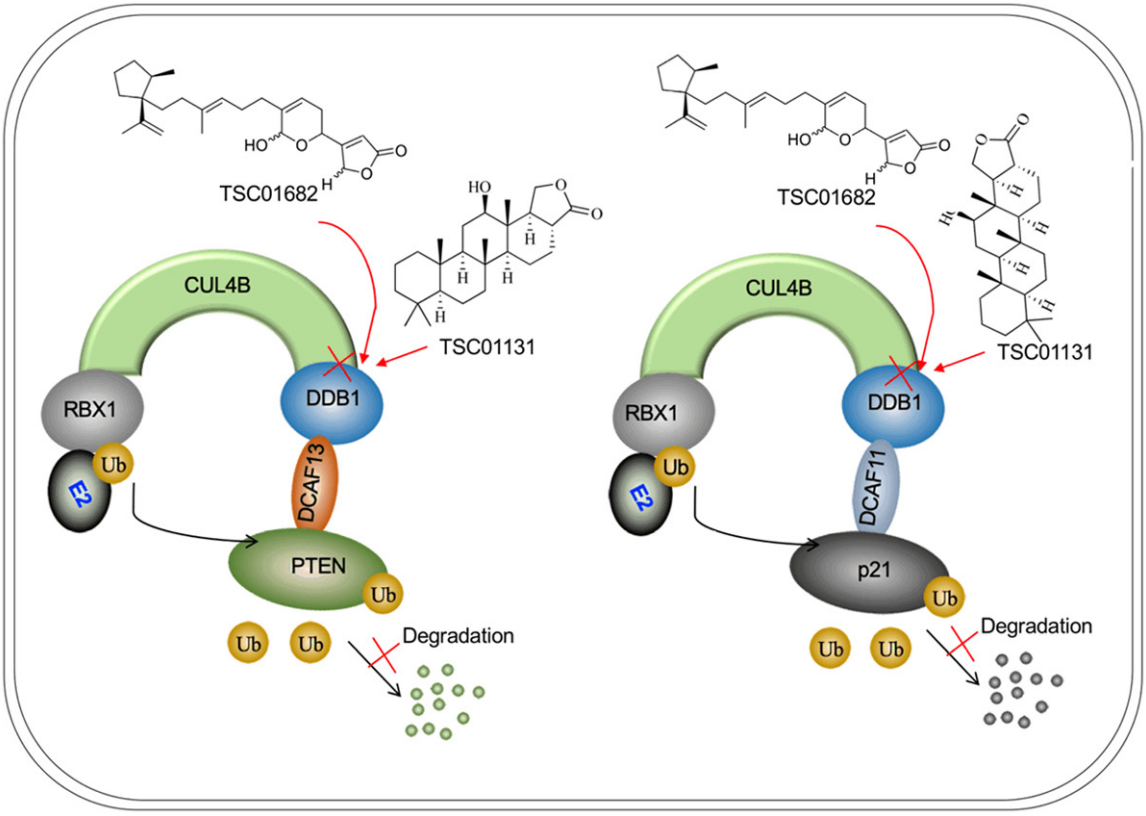

Figure 6. A schematic diagram of TSC01682 in human osteosarcoma cells. The CUL4B-DDB1 interaction provides a scaffold for the assembly of DCAF11 and DCAF13, which forms two separate CRL4B E3 ligases termed CRL4B^{DCAF11} and CRL4B^{DCAF13}. These two E3 ligases can ubiquitinate p21 and PTEN, respectively. The overexpression of CUL4B in human osteosarcoma cells increases CRL4B^{DCAF11} and CRL4B^{DCAF13} activities and causes the degradation of p21 and PTEN, leading to the occurrence of tumorigenesis. Two small molecules, TSC01682 and TSC01131, can prevent the CUL4B-DDB1 interaction, cause the disassociation of CRL4B complexes and lead to the accumulation of p21 and PTEN, eventually inhibiting tumor cell growth.

that are much more active. Another issue with these compounds is their cytotoxicities in normal cells, which may also be eliminated because normal cells also express CUL4 and DDB1. To address this possibility, we also used TSC01682 to treat three noncancerous cell lines, including a normal colon cell line CCD-18Co, a normal immortalized human ovarian cell line IOSE29 and an osteoblast cell line hFOB1.19 with TSC01682. Our results suggested that TSC01682 treatment caused nearly 30%-40% of growth inhibition in these noncancerous cells compared to nearly 80% reduction in Saos2 cells (Supplementary Figure 6). These results suggested that TSC01682 also had severe cytotoxicity in noncancerous cells instead of only selectively eliminating tumor cells, which may limit its use in clinical trials in the future. Another limitation of this study is that we did not use any chemotherapeutic drug as a control to compare its cytotoxicity with TSC01682 in tumor cells. Chemotherapeutic drugs often induce resistance after a period of treatment. Our *in vivo* data showed that TSC01682 could significantly eliminate tumors after 30 days of treatment, and we did not observe chemoresistance at this time point. In clinical treatment, it is a preliminary strategy to combine different chemotherapeutic drugs conferring drug resistance. We will evaluate the chemoresistance of these compounds as well as the combined effects of TSC01682 with other commercially chemotherapeutic drugs in animal models.

After treatment with TSC01682 and TSC01131 *in vitro* and *in vivo*, we observed a significant decrease in protein levels of CRL4B E3 ligase components but not their mRNA levels (Supplementary Figures 2 and 3). However, we

did not observe significant changes in CUL4B and DDB1 protein levels after small molecule treatments in yeast cells (**Figure 1C**). These interesting phenomenon implied that protein modifications might occur after small molecule treatments in human cells because TSC01682 and TSC01131 should only disrupt the interaction between CUL4B and DDB1 instead of causing their degradation. Both TSC01682 and TSC01131 treatment caused the same results, which excluded the possibility of small molecule specific degradation. A very likely cause was that small molecule treatments prevented the direct binding of DDB1 and CUL4B, which caused their exposure and then they were recognized and modified by other proteins, eventually leading to their degradation. Comparing the differences between yeast cells and human osteosarcoma cells, we speculated that proteins that could modify DDB1 and CUL4B had no homologous proteins in yeast, so it only caused significant degradation in osteosarcoma cells but not in yeast. The well-known posttranslational modifications include phosphorylation, ubiquitination, phosphorylation, acetylation, methylation, glycosylation, and sumoylation [26, 27]. After searching for commercial antibodies for CRL4B E3 components, we did not find any antibody to detect their modifications. Thus, we cannot reveal the mechanisms underlying protein degradation after TSC01628 and TSC01131 treatments at this time.

In summary, our study identified six candidate compounds that could block the CUL4B-DDB1 interaction. TSC01682 exhibited the most potent cytotoxicity to inhibit the growth of yeast cells and osteosarcoma cells that overexpressed CUL4B and DDB1. TSC01682 affected the assembly of CRL4B E3 ligases and caused the accumulation of their substrates p21 and PTEN, eventually leading to tumor cell growth inhibition.

Acknowledgements

We thank Dr. Zhi Chen for his help to design the experiments and carefully revising the manuscript.

Disclosure of conflict of interest

None.

Address correspondence to: Drs. Bin Chen and Hantao Wang, Department of Orthopaedics, Renji Hospital, School of Medicine, Shanghai Jiao Tong University, Shanghai 200006, China. E-mail: chnbn2003@126.com (BC); odowang@163.com (HTW)

References

[1] Enchev RI, Schulman BA and Peter M. Protein neddylation: beyond cullin-RING ligases. Nat Rev Mol Cell Biol 2015; 16: 30-44.

[2] Chen Z, Sui J, Zhang F and Zhang C. Cullin family proteins and tumorigenesis: genetic association and molecular mechanisms. J Cancer 2015; 6: 233-242.

[3] Jang SM, Redon CE and Aladjem MI. Chromatin-bound cullin-ring ligases: regulatory roles in DNA replication and potential targeting for cancer therapy. Front Mol Biosci 2018; 5: 19.

[4] Brown JS and Jackson SP. Ubiquitylation, neddylation and the DNA damage response. Open Biol 2015; 5: 150018.

[5] Jackson S and Xiong Y. CRL4s: the CUL4-RING E3 ubiquitin ligases. Trends Biochem Sci 2009; 34: 562-570.

[6] Jin J, Arias EE, Chen J, Harper JW and Walter JC. A family of diverse Cul4-Ddb1-interacting proteins includes Cdt2, which is required for S phase destruction of the replication factor Cdt1. Mol Cell 2006; 23: 709-721.

[7] Chen Z, Wang K, Hou C, Jiang K, Chen B, Chen J, Lao L, Qian L, Zhong G, Liu Z, Zhang C and Shen H. CRL4B(DCAF11) E3 ligase targets p21 for degradation to control cell cycle progression in human osteosarcoma cells. Sci Rep 2017; 7: 1175.

[8] Chen LC, Manjeshwar S, Lu Y, Moore D, Ljung BM, Kuo WL, Dairkee SH, Wernick M, Collins C and Smith HS. The human homologue for the caenorhabditis elegans cul-4 gene is amplified and overexpressed in primary breast cancers. Cancer Res 1998; 58: 3677-3683.

[9] Wang Y, Zhang P, Liu Z, Wang Q, Wen M, Wang Y, Yuan H, Mao JH and Wei G. CUL4A overexpression enhances lung tumor growth and sensitizes lung cancer cells to erlotinib via transcriptional regulation of EGFR. Mol Cancer 2014; 13: 252.

[10] Shiyanov P, Nag A and Raychaudhuri P. Cullin 4A associates with the UV-damaged DNA-binding protein DDB. J Biol Chem 1999; 274: 35309-35312.

[11] Hung MS, Mao JH, Xu Z, Yang CT, Yu JS, Harvard C, Lin YC, Bravo DT, Jablons DM and You L. Cul4A is an oncogene in malignant pleural mesothelioma. J Cell Mol Med 2011; 15: 350-358.

[12] Song B, Zhan H, Bian Q and Li J. Knockdown of CUL4B inhibits proliferation and promotes apoptosis of colorectal cancer cells through suppressing the Wnt/beta-catenin signaling pathway. Int J Clin Exp Pathol 2015; 8: 10394-10402.

[13] Pan WW, Zhou JJ, Yu C, Xu Y, Guo LJ, Zhang HY, Zhou D, Song FZ and Fan HY. Ubiquitin E3 ligase CRL4(CDT2/DCAF2) as a potential chemotherapeutic target for ovarian surface epithelial cancer. J Biol Chem 2013; 288: 29680-29691.

[14] He YM, Xiao YS, Wei L, Zhang JQ and Peng CH. CUL4B promotes metastasis and proliferation in pancreatic cancer cells by inducing epithelial-mesenchymal transition via the Wnt/beta-catenin signaling pathway. J Cell Biochem 2018; 119: 5308-5323.

[15] Liu H, Lu W, He H, Wu J, Zhang C, Gong H and Yang C. Inflammation-dependent overexpression of c-Myc enhances CRL4(DCAF4) E3 ligase activity and promotes ubiquitination of ST7 in colitis-associated cancer. J Pathol 2019; 248: 464-475.

[16] Nishitani H, Shiomi Y, Iida H, Michishita M, Takami T and Tsurimoto T. CDK inhibitor p21 is degraded by a proliferating cell nuclear antigen-coupled Cul4-DDB1Cdt2 pathway during S phase and after UV irradiation. J Biol Chem 2008; 283: 29045-29052.

[17] Li B, Jia N, Kapur R, Chun KT. Cul4A targets p27 for degradation and regulates proliferation, cell cycle exit, and differentiation during erythropoiesis. Blood 2006; 107: 4291-4299.

[18] Wang H, Zhai L, Xu J, Joo HY, Jackson S, Erdjument-Bromage H, Tempst P, Xiong Y and Zhang Y. Histone H3 and H4 ubiquitylation by the CUL4-DDB-ROC1 ubiquitin ligase facilitates cellular response to DNA damage. Mol Cell 2006; 22: 383-394.

[19] Chen Z, Zhang W, Jiang K, Chen B, Wang K, Lao L, Hou C, Wang F, Zhang C and Shen H. MicroRNA-300 regulates the ubiquitination of PTEN through the CRL4B(DCAF13) E3 ligase in osteosarcoma cells. Mol Ther Nucleic Acids 2018; 10: 254-268.

[20] Taran SJ, Taran R and Malipatil NB. Pediatric osteosarcoma: an updated review. Indian J Med Paediatr Oncol 2017; 38: 33-43.

[21] Zhang Y, Yang J, Zhao N, Wang C, Kamar S, Zhou Y, He Z, Yang J, Sun B, Shi X, Han L and Yang Z. Progress in the chemotherapeutic treatment of osteosarcoma. Oncol Lett 2018; 16: 6228-6237.

[22] Liu L and Huang M. Essential role of the iron-sulfur cluster binding domain of the primase regulatory subunit Pri2 in DNA replication initiation. Protein Cell 2015; 6: 194-210.

[23] He F, Cheng XM and Gu WL. Effects of cullin 4B on the proliferation and invasion of human gastric cancer cells. Mol Med Rep 2018; 17: 4973-4980.

[24] Sui X, Zhou H, Zhu L, Wang D, Fan S and Zhao W. CUL4A promotes proliferation and metastasis of colorectal cancer cells by regulating H3K4 trimethylation in epithelial-mesenchymal transition. Onco Targets Ther 2017; 10: 735-743.

[25] Yu R, Cai L, Chi Y, Ding X and Wu X. miR377 targets CUL4A and regulates metastatic capability in ovarian cancer. Int J Mol Med 2018; 41: 3147-3156.

[26] Duan G, Walther D. The roles of post-translational modifications in the context of protein interaction networks. PLoS Comput Biol 2015; 11: e1004049.

[27] Santos AL, Lindner AB. Protein posttranslational modifications: roles in aging and age-related disease. Oxid Med Cell Longev 2017; 2017: 5716409.

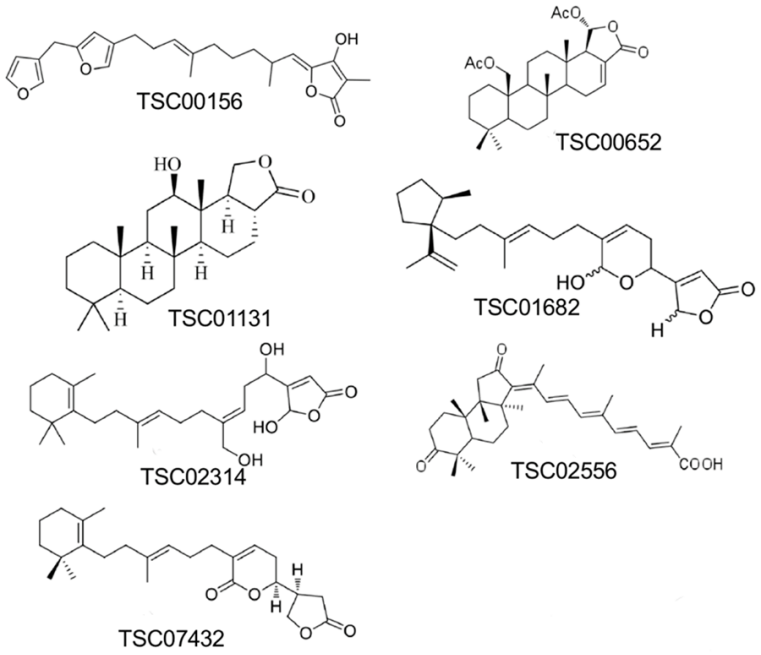

Supplementary Figure 1. Chemical structures of seven candidate compounds that specifically disrupt the DDB1-CUL4B interaction. A total of seven small molecules that disrupted the DDB1-CUL4B interaction were obtained using an *in vitro* HTS method. The chemical structures of these seven compounds including TSC00156, TSC00652, TSC01131, TSC01682, TSC02314, TSC02556, and TSC07432 were shown.

Supplementary Table 1. *P* values of **Figure 1C**

	0	1	2	4	8	16	32	64 uM
Untreated vs TSC00156	0.73	0.27	0.042 (*)	0.034 (*)	0.0092 (**)	0.0034 (**)	0.0028 (**)	0.001 (***)
Untreated vs TSC00652	0.91	0.8	0.26	0.079	0.013 (*)	0.0074 (**)	0.0021 (**)	0.0019 (**)
Untreated vs TSC01131	0.48	0.31	0.055	0.016 (*)	0.0038 (**)	0.00076 (***)	0.00032 (***)	0.00036 (***)
Untreated vs TSC01682	0.74	0.017 (*)	0.0067 (**)	0.0043 (**)	0.00084 (***)	0.00036 (***)	0.00014 (***)	0.00013 (***)
Untreated vs TSC02314	0.36	0.44	0.021 (*)	0.021 (*)	0.0035 (**)	0.0014 (**)	0.0013 (**)	0.00085 (***)
Untreated vs TSC02556	0.99	0.57	0.53	0.23	0.065	0.03 (*)	0.011 (*)	0.0042 (**)
Untreated vs TSC07432	0.98	0.63	0.079	0.0076 (**)	0.002 (**)	0.00098 (***)	0.0084 (**)	0.00053 (***)
TSC01682 vs TSC00156	0.41	0.032 (*)	0.092	0.028 (*)	0.011 (*)	0.0036 (**)	0.0013 (**)	0.00043 (***)
TSC01682 vs TSC00652	0.66	0.0076 (**)	0.0094 (**)	0.012 (*)	0.0051 (**)	0.0019 (**)	0.00023 (***)	0.00049 (***)
TSC01682 vs TSC01131	0.73	0.055	0.081	0.16	0.066	0.027 (*)	0.02 (*)	0.0089 (**)
TSC01682 vs TSC02314	0.65	0.072	0.22	0.13	0.11	0.0081 (**)	0.0055 (**)	0.004 (**)
TSC01682 vs TSC02556	0.39	0.014 (*)	0.0091 (**)	0.0063 (**)	0.00023 (***)	0.00089 (***)	0.00034 (***)	0.00038 (***)
TSC01682 vs TSC07432	0.84	0.75	0.6	0.33	0.3	0.061	0.0046 (**)	0.013 (*)

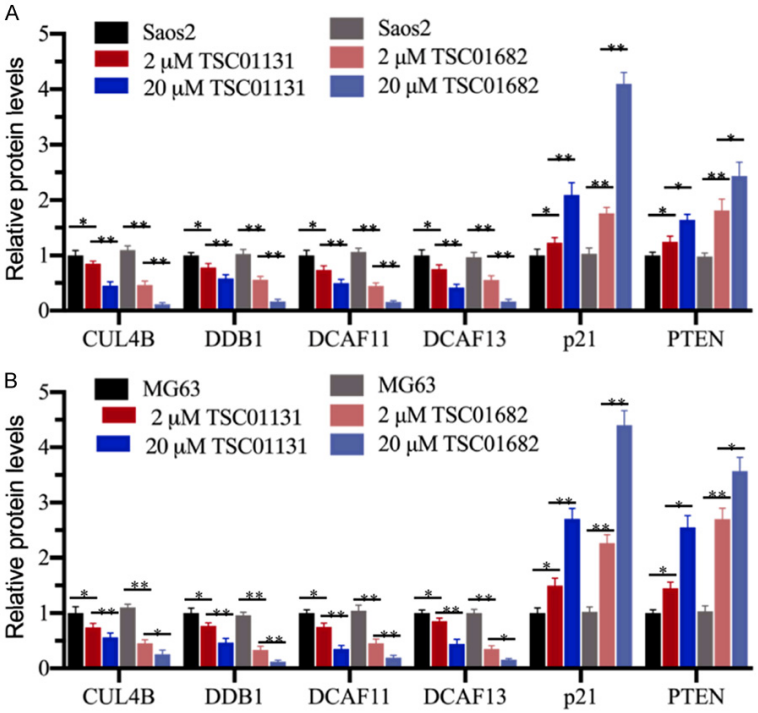

Supplementary Figure 2. The quantification results of CRL4B E3 ligase component levels after TSC01682 treatment. The protein signal intensities in **Figure 2C** and **2D** were normalized to those of GAPDH. The ratios of CUL4B/GAPDH, DDB1/GAPDH, DCAF11/GAPDH, DCAF13/GAPDH, p21/GAPDH and PTEN/GAPDH in Saos2 (A) and MG63 (B) cells were defined as the baseline. $*P < 0.05$ and $**P < 0.01$.

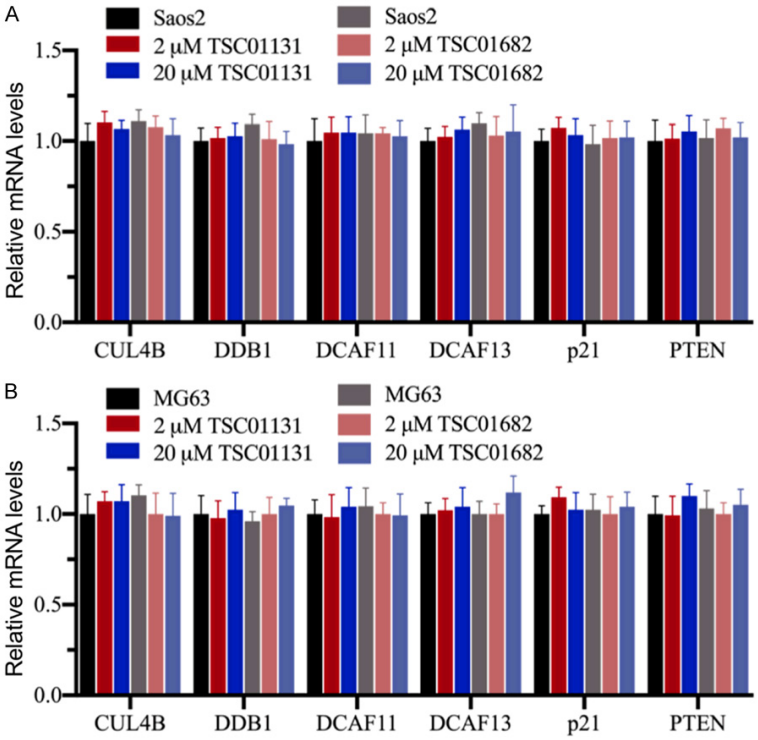

Supplementary Figure 3. TSC01682 treatment did not change the mRNA levels of CRL4B E3 ligase components and their substrates. Saos2 (A) and MG63 cells (B) were treated with 2 μM and 20 μM TSC01682 and TSC01131 for 12 h, and the mRNA levels of *CUL4B*, *DDB1*, *DCAF11*, *DCAF13*, *p21* and *PTEN* were examined. The mRNA levels of these genes in untreated Saos2 and MG63 cells were defined as the baseline.

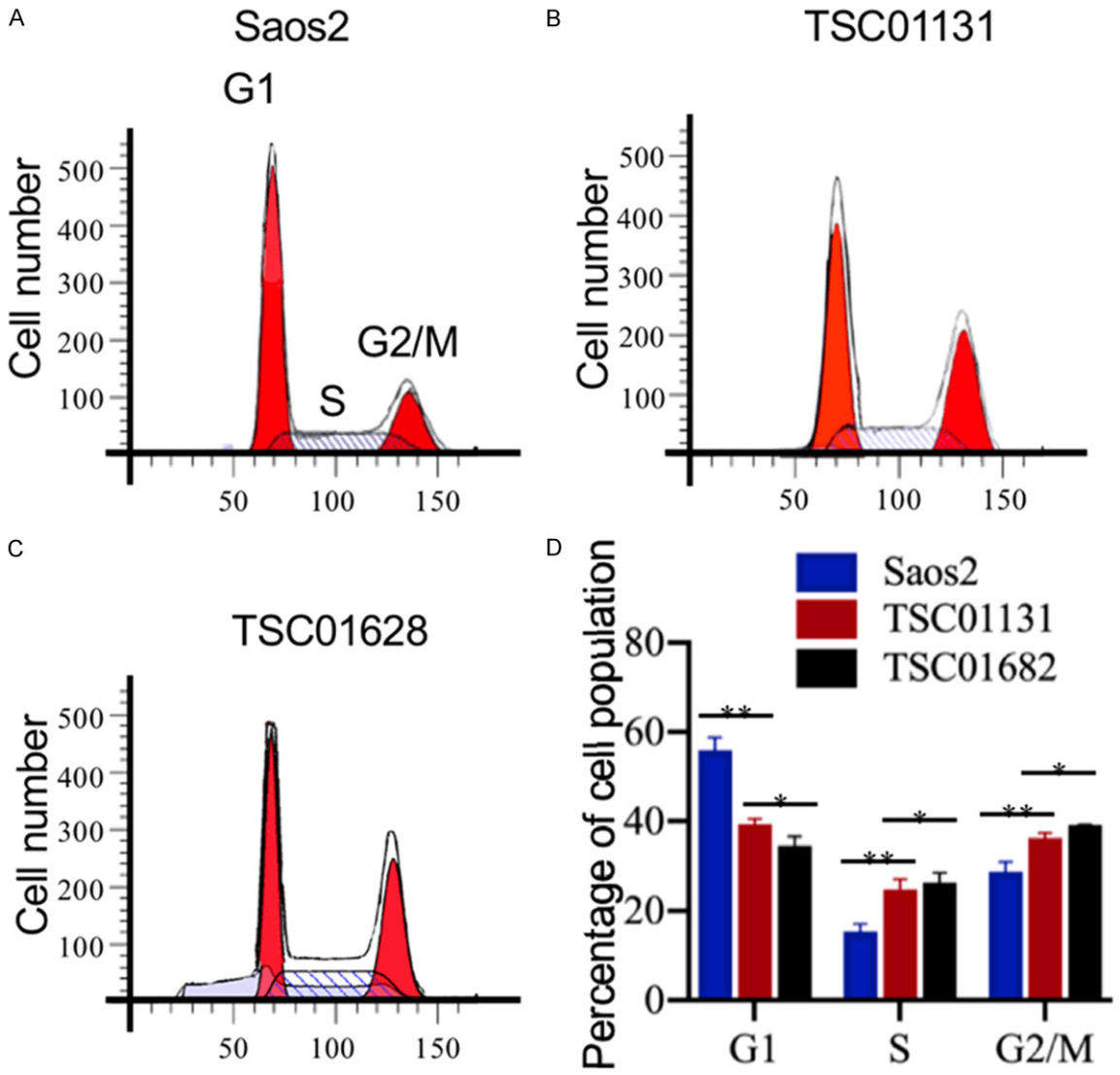

Supplementary Figure 4. TSC01682 treatment resulted in cell cycle S phase arrest. Saos2 cells (A), and Saos2 cells treated with TSC01131 (B) and TSC01682 (C) were subjected to flow cytometry analysis to investigate the cell cycle distributions. The cell cycle distributions from (A) to (C) were quantified in (D).

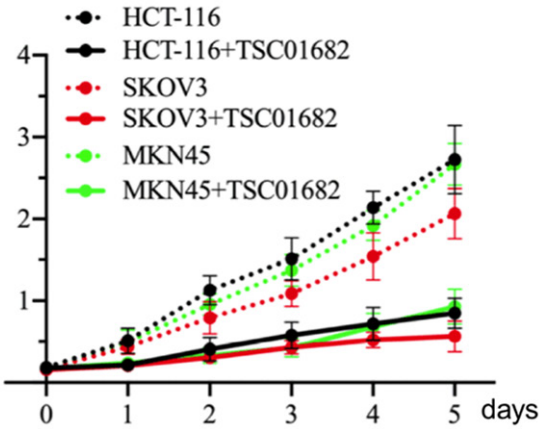

	0	1 day	2 day	3 day	4 day	5 day
HCT-116 vs HCT-116+TSC01682	0.81	0.033 (*)	0.0056 (**)	0.0062 (**)	0.00098 (***)	0.00091 (***)
SKOV3 vs SKOV3+TSC01682	0.88	0.019 (*)	0.016 (*)	0.003 (**)	0.0044 (**)	0.002 (**)
MKN45 vs MKN45+TSC01682	0.95	0.042 (*)	0.027 (*)	0.0019 (**)	0.00096 (***)	0.00083 (***)

Supplementary Figure 5. TSC01682 significantly inhibited the growth of tumor cells overexpressing *CUL4A* or *CUL4B*. *Cell proliferation assay. Three tumor cell lines, HCT-116, SKOV3 and MKN45,* were grown in DMEM medium supplemented with or without 10 μM TSC01682 for 5 days. Cells were collected daily and subjected to cell viability assessment using an MTT assay. The data of all treatments at different time points were analyzed using a two-sided Student's *t* test to compare their significance. **P* < 0.05, ***P* < 0.01 and ****P* < 0.001.

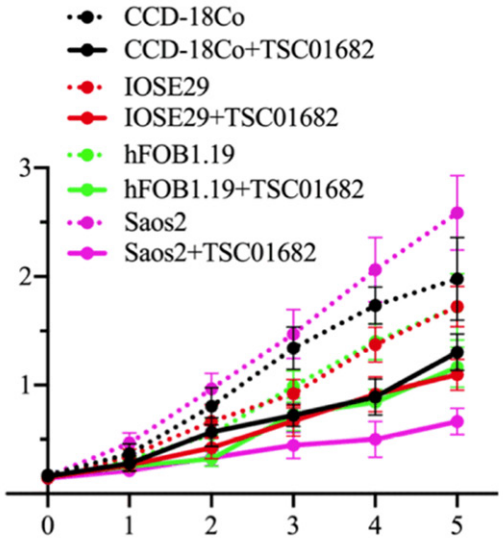

	0	1 day	2 day	3 day	4 day	5 day
CCD-18Co vs CCD-18Co+TSC01682	0.57	0.25	0.13	0.0084 (**)	0.0037 (**)	0.026 (*)
IOSE29 vs IOSE29+TSC01682	0.87	0.18	0.085	0.086	0.025 (*)	0.0097 (**)
hFOB1.19 vs hFOB1.19+TSC01682	0.59	0.16	0.057	0.097	0.016 (*)	0.055
Saos2 vs Saos2+TSC01682	0.42	0.014 (*)	0.0024 (**)	0.0022(**)	0.0012 (**)	0.00079 (***)

Supplementary Figure 6. TSC01682 significantly inhibits the growth of normal cells. *Three normal cell lines,* CCD-18Co, IOSE29 and hFOB1.19, were grown in DMEM supplemented with or without 10 μM TSC01682 for 5 days. Cells were collected daily and subjected to cell viability assessment using an MTT assay. The data of all treatments at different time points were analyzed using a two-sided Student's *t* test to compare their significance. **P* < 0.05, ***P* < 0.01 and ****P* < 0.001.